Spectral and lasing investigations of garnets with Yb^{3+} ions

G. A. Bogomolova, D. N. Vylegzhanin, and A. A. Kaminskiĭ

Crystallography Institute, USSR Academy of Sciences

(Submitted April 15, 1975)
Zh. Eksp. Teor. Fiz. **69**, 860–874 (September 1975)

A set of spectral and lasing investigations is carried out on a large number of ytterbium-activated garnets, in which the tetrahedral and octahedral crystallographic positions are filled either with like ions ($Y_3Al_5O_{12}$, $Y_3Ga_5O_{12}$, $Gd_3Ga_5O_{12}$, $Lu_3Al_5O_{12}$, $Lu_3Ga_5O_{12}$) or unlike ions ($Gd_3Sc_2Al_3O_{12}$ and $Lu_3Sc_2Al_3O_{12}$). Stimulated emission was observed in these compounds, and the values of its main parameters are determined. Temperature investigations of the laser emission of $Y_3Al_5O_{12}$ crystals co-activated with ytterbium, chromium, and neodymium (the last two serving as sensitizers) at ≈200°K have revealed simultaneous lasing of the Yb^{3+} ions on the *D* line of the $^2F_{5/2}\rightarrow{}^2F_{7/2}$ transition and of Nd^{3+} ion on the lines *A* and *B* of the $^4F_{3/2}\rightarrow{}^4I_{11/2}$ transition. The absorption and luminescence of the Yb^{3+} ions in the crystals $Y_3Al_5O_{12}$ and $Lu_3Al_5O_{12}$ are investigated in detail. The Stark splitting of the $^2F_{5/2}$ and $^2F_{7/2}$ multiplets as well as the probabilities of the radiative transitions between these states are determined. The change of the luminescence lifetime and of the widths and positions of the luminescence lines with changing temperature are investigated. The results are interpreted in the approximate model of electron-phonon interaction with allowance for the singularities of the distribution of the density of the impurity-active phonons in aluminum garnets.

PACS numbers: 78.45.+h, 78.60.Dg, 71.70.Ej

INTRODUCTION

Much attention has been paid recently in the physics of activated media to the Yb^{3+} ion. Its only term ^2F, belonging to the 4f configuration, is split by spin-orbit interaction into two multiplets $^2F_{5/2}$ and $^2F_{7/2}$, the energy gap between them corresponds to the near IR band ($\Delta E \approx 10\,000\ cm^{-1}$). The particular interest evoked by media with Yb^{3+} ions is caused to a considerable extent by the fact that they provide a valuable possibility of a comprehensive investigation of many various physical phenomena observed in activated systems. This pertains in particular to laser crystals, where use can be made of the entire arsenal of the experimental methods of modern spectroscopy, including analysis of the luminescence, absorption stimulated-emission (SE), and of resonant Raman scattering spectra. A study of these phenomena is of great interest to solid-state physics, and some of these phenomena can be of practical significance. Among the latter, first place is occupied by IR lasing[1-6] and sensitization of the luminescence of a number of TR^{3+} ions,[7-9] and also by cooperative effects that lead to conversion of IR into visible radiation.[10-12]

Owing the simplicity of the energy level scheme of the Yb^{3+} ions, media activated with it can serve as good model objects for the study of a large number of effects. Of exceptional interest among these effects are various manifestations of electron-phonon interaction (EPI). The absence of cross-relaxation and nonradiative luminescence-quenching channels permits an investigation of the migration of the excitation energy between the activator centers (AC) and luminescence quenching by extraneous impurities[13,14] in "pure" form. These processes influence strongly the kinetics of the decay of the excited state1) and, in final analysis, the spectral and lasing parameters of the medium.

The present paper is devoted to an experimental and theoretical study of the main physical phenomena that cause stimulated emission of Yb^{3+} ion in crystals with garnet structure ($O_h^{10}-Ia3d$) or phenomena accompanying this emission. The primary task of these studies was to obtain information concerning the effect of EPI on the spectral characteristics of a number of garnets with Yb^{3+} ions and to assess the possibility of developing on their basis effective lasers emitting in the 1-μ region.

CRYSTALS, EXPERIMENTAL TECHNIQUE, AND RESEARCH METHODS

In our comprehensive investigations we used a large number of garnets with Yb^{3+}, including new ones, in which the tetrahedral (S_4) and octahedral (C_{3i}) crystallographic positions are filled either with like (Al^{3+} or Ga^{3+}, viz., $Y_3Al_5O_{12}$, $Y_3Ga_5O_{12}$, $Gd_3Ga_5O_{12}$, $Lu_3Al_5O_{12}$, and $Lu_3Ga_5O_{12}$) and unlike ions (Al^{3+} and Sc^{3+}, viz., $Gd_3Sc_2Al_3O_{12}$ and $Lu_3Sc_2Al_3O_{12}$).2) The content of ytterbium and of other specially introduced ions Cr^{3+} and Nd^{3+}) in these crystals, grown by melt methods (inactive losses not worse than $0.1\ cm^{-1}$) was determined either by chemical means or by x-ray fluorescence methods (using external standards). In some samples, the impurity concentration was estimated also by absorption measurements. For a detailed study of the main characteristics of the absorption, luminescence, and SE of the Yb^{3+} ions we chose the crystals $Y_3Al_5O_{12}$ and $Lu_3Al_5O_{12}$.

Most spectroscopic measurements were made by universally known methods using high-resolution spectral instruments. In the lasing experiments we used a high-efficiency elliptic illuminator with a type IFP-400 flash lamp. The active element, placed in a glass tubular cryostat, was cooled either with liquid nitrogen or with its vapor. The confocal optical cavity used by us ($R \approx 576$ mm) was produced by external spherical interference mirrors with $\tau \approx 1\%$ in the 1.02–1.07 μ range. The lasing crystal was connected to the resonator mirrors by special quartz lightpipes. The spectral composition of the SE was registered photographically, the reference spectrum being the emission of a lamp with a hollow iron cathode. The threshold excitation energy (E_{thr}) of the individual SE lines was measured with an FD 9E 111 photodiode placed in the focal region of a DFS-8 spectrograph, and with an S1-16 oscilloscope. The temperature was monitored in all the experiments with a copper-constantan or chromel-alumel thermocouple directly fastened to the crystal, and with an F116/2 millivoltmeter.

The list of the investigated crystals, their dimensions, the activator concentrations, and the results of the spectral and lasing measurements are listed in Table I.

INITIAL PREMISES AND PROBLEMS OF THE THEORY

1. Optical spectra of Yb^{3+} in garnets. The interpretation of the optical spectra of Yb^{3+} in the wavelength region ≈1 μ is made difficult by the presence of an intense electron-vibrational structure (EVS). This was the cause of appreciable discrepancies in the previously proposed[15-17] crystalline splitting of the states of Yb^{3+} in garnets. In[15], the absorption spectrum of $Y_3Al_5O_{12}:Yb^{3+}$, obtained at 300°K, was compared with the luminescence spectrum obtained at 77°K. The energy values 0, 140, 390, and 620 cm^{-1} were proposed for the Stark components of the $^2F_{7/2}$ multiplet. These data contradict the measured values of the magnetic susceptibility of garnets with Yb^{3+} [15,16], according to which the ground state Stark components have an energy not less than 500 cm^{-1}.

Koningstein[16] investigated the spectra of $Y_3Al_5O_{12}$ and $Gd_3Ga_5O_{12}$ with Yb^{3+} ions; he interpreted the spectra in a crystal-field model corresponding to tetragonal symmetry of the AC. The choice of the zero-phonon lines (ZPL) in the absorption and luminescence spectra was made without convincing justification, and the good agreement obtained between the theoretical values of the Stark splitting in both crystals with experiment is the only argument that can be advanced in favor of the constructed level scheme ($Y_3Al_5O_{12}$—Yb^{3+}, $^2F_{7/2}$: 0, 388, 613, and 776 cm^{-1}). Yet more accurate calculations[20,21] with allowance for the real symmetry of the Yb^{3+} position in the garnets agree with cited data of[18,19] and do not confirm the existence of an electronic level with ≈400 cm^{-1} energy. The most justified level schemes of Yb^{3+} in aluminum garnets were obtained in[17], where the ZPL were separated in accord with the results of a detailed comparison of the luminescence and absorption spectra. Certain conclusions of this paper, however, cannot be regarded as final. Recently obtained data make it possible to refine these conclusions.

TABLE I. Spectral and lasing characteristics of garnets with Yb^{3+} ions.

Crystal* (length and diameter of laser element in mm)	Laser ion	T, K	λ_g^{**}, Å	Lasing Transition	$E_{п}^{***}$, J	$\Delta\nu_{lum}^{****}$, cm^{-1}	E_c^{*****}, cm^{-1}	$\Delta\nu_g^{******}$, cm^{-1}
$Y_3Al_5O_{12}$–0,7 Yb^{3+} (24; 6)	Yb^{3+}	77	10293	$^2F_{5/2}\rightarrow{}^2F_{7/2}$	9	≈7	612	≈1
$Y_3Al_5O_{12}$: 0,8 Nd^{3+}–2,0 Yb^{3+} (24; 6)	Yb^{3+}	77	10293	$^2F_{5/2}\rightarrow{}^2F_{7/2}$	4.5	≈7	612	≈1
	»	200	10297	»	145	25	≈612	≈4
	Nd^{3+}	200	10612Б	$^4F_{3/2}\rightarrow{}^4I_{11/2}$	160	≈2	2005	≈1
$Y_3Al_5O_{12}$: 0,5 Cr^{3+}; 0,8 Nd^{3+}–2,0 Yb^{3+} (35; 6)	Yb^{3+}	77	10293	$^2F_{5/2}\rightarrow{}^2F_{7/2}$	2	≈7	612	≈1
	»	210	10298	»	115	25	≈612	≈4
	»	220	–	»	≈175	–	≈612	–
	Nd^{3+}	210	10612Б	$^4F_{3/2}\rightarrow{}^4I_{11/2}$	100	3	2005	≈1
	»	210	10638A	»	120	4	2110	≈1
$Y_3Ga_5O_{12}$: 1,5 Nd^{3+}–2,0 Yb^{3+} (15; 5)	Yb^{3+}	77	10233	$^2F_{5/2}\rightarrow{}^2F_{7/2}$	2	≈8	–	≈1
$Gd_3Ga_5O_{12}$: 2,0 Nd^{3+}–2,0 Yb^{3+} (15; 5)	Yb^{3+}	77	10232	$^2F_{5/2}\rightarrow{}^2F_{7/2}$	2.5	≈8	–	≈1
$Gd_3Sc_2Al_3O_{12}$: : 1,5 Nd^{3+}–2,0 Yb^{3+} (20; 5,5)	Yb^{3+}	77	10299	$^2F_{5/2}\rightarrow{}^2F_{7/2}$	8	≈13	–	≈1.5
$Lu_3Al_5O_{12}$–2,0 Yb^{3+} (30; 6)	Yb^{3+}	77	10294	$^2F_{5/2}\rightarrow{}^2F_{7/2}$	1.5	≈7	621	≈1
	»	175	10297	»	35	21	621	≈3
$Lu_3Al_5O_{12}$: 1,0 Nd^{3+}–2,0 Yb^{3+} (15; 5)	Yb^{3+}	77	10294	$^2F_{5/2}\rightarrow{}^2F_{7/2}$	1	≈7	621	≈1
$Lu_3Al_5O_{12}$: 0,1 Cr^{3+}; 0,5 Nd^{3+}–5,0 Yb^{3+} (31; 5)	Yb^{3+}	77	10294	$^2F_{5/2}\rightarrow{}^2F_{7/2}$	1.5	≈7	621	≈1
$Lu_3Ga_5O_{12}$: 1,5 Nd^{3+}–2,0 Yb^{3+} (25; 5)	Yb^{3+}	77	10230	$^2F_{5/2}\rightarrow{}^2F_{7/2}$	1.5	≈8	–	≈1
$Lu_3Sc_2Al_3O_{12}$: : 1,5 Nd^{3+}–2,0 Yb^{3+} (25; 6)	Yb^{3+}	77	10299	$^2F_{5/2}\rightarrow{}^2F_{7/2}$	5	≈13	–	≈1.5

*The end faces of the laser elements were plane-parallel within 7″. The lasing-ion and sensitizing-ion densities are given in at.%.

**Lasing wavelength measurement accuracy ±0.5 Å.

***The excitation threshold was recalculated in terms of the crystal length.

****At the 0.5 level.

*****Energy of the level at which the induced transition terminates.

******The lasing line width was measured at $E_{exc}/E_{thr}=3$.

2. Temperature dependence of E_{thr}. The expression for the threshold energy of the excitation of SE of Yb^{3+} ions can be obtained by solving the system of kinetic equations for a four-level laser scheme with low-lying final level. Assuming that the thermal equilibrium between the Stark components of each working state is established very rapidly and that the multiphonon nonradiative transition (NRT) $^2F_{5/2}\rightarrow{}^2F_{7/2}$ have low probability, we obtain

$$E_{\mathrm{thr}}(T)\sim\Delta\nu_{\mathrm{lum}}\left[1+C_0\frac{N_g'}{\Delta\nu_{\mathrm{lum}}}\right]\frac{1}{\beta_g}, \tag{1}$$

where

$$C_0=\frac{N_0}{\alpha}\Delta\nu_{\mathrm{lum}}\sigma_e,\quad \sigma_e=\frac{\lambda_g^2A}{4\pi^2n^2c\Delta\nu_{\mathrm{lum}}},\quad \beta_g=A\tau_{\mathrm{rad}}N_g, \tag{2}$$

A and $\Delta\nu_{lum}$ are the probability and line width of the spontaneous emission for the transition for which the SE is observed; σ_e and β_g are the effective cross section of the transition and the branching coefficient of the luminescence for this transition; τ_{rad} is the radiative lifetime of the $^2F_{5/2}$ state (in our case it is equal to τ_{lum}); α is the total-loss coefficient; N_g is the Stark-component population at which the induced transition (IT) begins, divided by the population of the $^2F_{5/2}$ multiplet; N_g' is the Stark-component population at which the IT ends, divided by the population of the ground state; N_0 is the ion density; n is the refractive index and c is the speed of light.

The three factors in (1) correspond to the three main factors that cause the temperature dependence of E_{thr}, namely the broadening of the ZPL, the growth of the population of the final working level, and the change of the luminescence branching coefficient for the line at the frequency of which the SE is obtained.

3. Temperature broadening and shift of spectral lines. The calculations performed in[22,23] have shown that the homogeneous component of the spectral-line width of TR^{3+}-ion lines in aluminum garnets, up to ≈500°K is due to one-phonon relaxation transitions. The presence of pronounced singularities of the effective phonon density function $\rho(\omega_{ph})$ can strongly influence the ZPL broadening of the corresponding frequency ω_{ph} is at resonance with an intramultiplet transition. Correlations between the relative broadenings of individual Stark components and the phonon-density peaks were noted in[24,25]. Allowance for the real form of the function (ω_{ph}) is of primary significance in the calcula-

tion of not only the temperature broadening but also of the shift of the spectral lines of the TR^{3+} ions[23,24].

The form of the function $\rho(\omega_{ph})$ can be determined from the form of the EVS. The weak EPI characteristic of the TR^{3+} ions favors this possibility, for in this case the entire observed EVS corresponds in the main to one-phonon transitions. In optical spectra of garnet-structure crystals with TR^{3+} ion impurities, a sufficiently intense EVS is observed only for Yb^{3+} ions. The cause of this phenomenon has not been determined in detail as yet, but its presence agrees with the long-noted fact that various manifestations of EPI are enhanced in the case of the outermost members of the TR^{3+} ion series.[26] The problem of determining the form of the function $\rho(\omega_{ph})$ in aluminum garnets from the optical spectra of the Yb^{3+} ion can serve as a topic for a separate study. For the time being we use these spectra only for a qualitative estimate of the role of various phonons in the line broadening and shift.

The line broadening due to one-phonon relaxation transitions is described by the expression

$$\Delta\nu_{m,k}=\Delta E_m+\Delta E_k,$$

$$\Delta E_{m,k}=\sum_{i\neq m,k}\beta_{i\to m,k}\rho(\omega_{i\to m,k})\left[\bar{n}(\omega_{i\to m,k})+{}^1/_2\pm{}^1/_2\right], \tag{3}$$

where $E_{m,k}$ are values of the energy of the initial and final levels of the considered optical transition; $\beta_{i\to mk}$ is a factor that includes, besides the physical parameters of the crystal, also the matrix element of the EPI operator for the corresponding relaxation transition; $\bar{n}(\omega)$ is the occupation number of phonons of frequency ω; the plus sign is taken for transitions that lead to phonon emission, and the minus sign for transition with phonon absorption. The relative value of the coefficient $\beta\rho(\omega_{ph})$, as indicated, is determined mainly by the value of $\rho(\omega_{i\to m,k})$.

To interpret the spectral-line shift due to EPI it is advantageous to divide it into two parts, one corresponding to the shifts of the initial and final levels relative to the gravity centers of their multiplets, and the second to the mutual shift of the latter. To explain the first effect it is necessary to consider the virtual transitions from each of these levels to all the states of its own multiplet. To explain the second it is necessary to consider intermultiplet virtual transitions. The intense EVS makes it impossible to estimate experimentally the Stark splittings and to determine the gravity centers of the two Yb^{3+} multiplets in a sufficiently broad temperature interval. Since, however, the distance between these multiplets greatly exceeds their Stark splitting, we shall henceforth neglect the contribution of the intermultiplet virtual transitions and the shift of the Yb^{3+} lines.

The intramultiplet temperature shift of the electronic level is described by the expression

$$E_m(T)-E_m(0)=-\sum_{l\neq m}\alpha_{ml}P\int_0^{\infty}\rho(\omega)\frac{\Delta_{ml}}{(\Delta_{ml}^2-\omega^2)}\bar{n}(\omega)d\omega, \tag{4}$$

where α is a coefficient that includes all the parameters that are independent of the frequency of the impurity-active phonons; $\Delta_{ml} = E_m - E_l$; P is the principle-value symbol for the improper integral. Calculations by formula (4) using the real form of the function $\rho(\omega_{ph})$ are quite laborious. The expression for the level shift becomes much simpler if it is assumed that the effect is due to interaction with crystal vibrations corresponding in the impurity-active phonon spectrum to a sharp peak at a certain frequency $\omega_{ph} = \omega'$. In this case we obtain from (4) the expression

$$E_m(T)-E_m(0)=-A\bar{n}(\omega')\sum_{l\neq m}\frac{1}{\Delta_{ml}^2-\omega'^2}, \tag{5}$$

in which the only temperature-dependent factor is $\bar{n}(\omega')$.

EXPERIMENTAL DATA AND THEIR DISCUSSION

1. Determination of the Stark splittings of the Yb^{3+} states. The absorption and luminescence spectra of the Yb^{3+} ions in $Y_3Al_5O_{12}$ and $Lu_3Al_5O_{12}$ are shown in Figs. 1 and 2. They can be used to determine reliably the frequencies of only two of the twelve ZPL corresponding

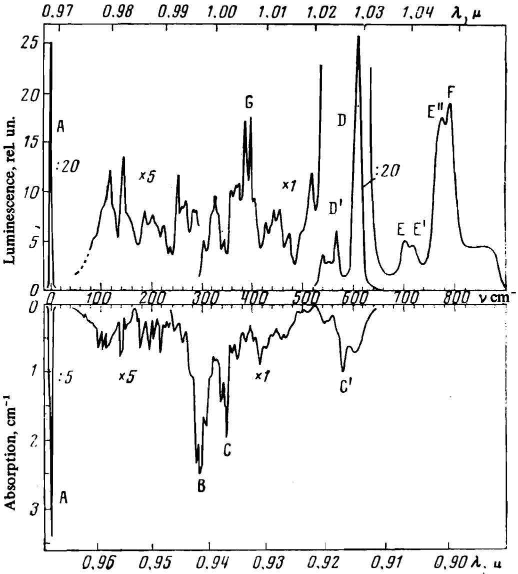

FIG. 1. Luminescence and absorption spectra of Yb^{3+} lines (≈1 at. %) in $Y_3Al_5O_{12}$ ($^2F_{5/2}\leftrightarrow{}^2F_{7/2}$) at 77°K with allowance for the corrections for the sensitivity of the photoreceiver (explanation in the text).

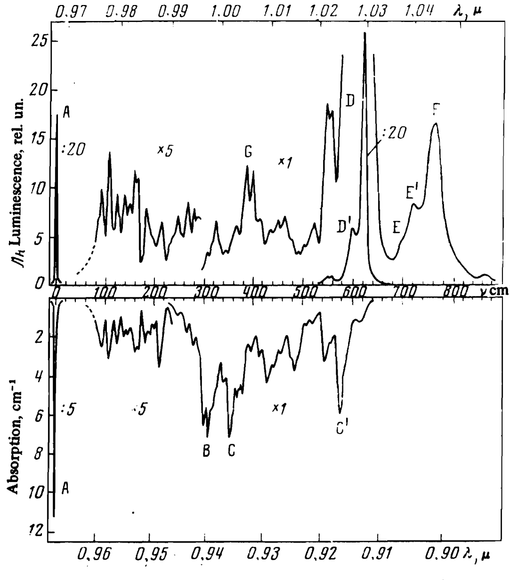

FIG. 2. Luminescence and absorption spectra of Yb^{3+} ions (≈3 at.%) in $Lu_3Al_5O_{12}$ ($^2F_{5/2}\leftrightarrow{}^2F_{7/2}$) at 77°K with allowance for corrections of the photoreceiver sensitivity.

to the $^2F_{5/2} \longleftrightarrow {}^2F_{7/2}$ transitions. These are lines A and D. The intensities of the remaining ZPL are low, and their separation from among the EVS peaks is a problem in itself.

Comparing the luminescence and absorption spectra in each of the crystals, it is easy to note in them a definite symmetry of the arrangement of the lines relative to the line A. Comparison of the luminescence spectra of the Yb^{3+} and Cr^{3+} ions in[3)] $Y_3Al_5O_{12}$ shows that the positions of a large number of lines agree well in these spectra. It can therefore be concluded that the entire EVS observed in the Yb^{3+} spectrum pertains to the one line A, and consequently from the shape of this line we can assess the spectral distribution of the effective density of the lattice vibrations $\rho(\omega_{ph})$. In both considered crystals this distribution is in general similar both with respect to the positions of the individual peaks and with respect to their relative intensities. A characteristic feature of the function $\rho(\omega_{ph})$ for aluminum garnets is the presence of two narrow and intense peaks G at frequencies close to 400 cm^{-1}. It would be incorrect to regard these lines as electronic, since they are observed also in the luminescence spectra of the ions Cr^{3+} and Mn^{4+},[27,28] although these ions occupy a different crystallographic position (C_{3i}).

To determine the positions of the purely electronic lines, we compare the luminescence and absorption spectra and single out the lines that have no twins symmetrical about the line A. Such lines are B and C in the absorption spectrum and D′, D, and F in the luminescence spectrum. An additional argument in favor of the electronic origin of these lines is that their positions relative to the line A changes noticeably (by 10–20 cm^{-1}) on going from one crystal to another, something that cannot be said concerning the positions of all the remaining peaks belonging to the EVS. For the latter, the mean squared frequency difference is only ≈ 4.5 cm^{-1} in luminescence (for 20 line pairs) and ≈ 5 cm^{-1} in absorption (for 26 line pairs). In addition, resonant Raman-scattering line peaks were observed at the frequencies corresponding to the energy distances of the lines D′, D, and F from the line A.[29] The Stark splitting schemes for the multiplets $^2F_{5/2}$ and $^2f_{7/2}$ in the crystals $Y_3Al_5O_{12}$ and $Lu_3Al_5O_{12}$ are shown in Fig. 3.

Wood[15] and Koningstein[16] assumed one of the ZPL to be C′ instead of C. Buchanan et al.[17] assigned this line to the EVS, assuming it to be a twin of the D′ line on the basis of the fact that in $Yb_3Al_5O_{12}$ the positions of these lines relative to A line coincide. In both crystals investigated by us the relative positions of these lines do not coincide. It is therefore clear that they are not twins. The absence of a twin of the C′ line from the luminescence spectrum is due to the fact that this spectrum falls in the region of intense ZPL. A detailed investigation of the luminescence spectrum in the region of lines D′ and D indeed shows the presence of a line whose position approximately coincides with that of C′. This is particularly noticeable in the $Y_3Al_5O_{13}:Yb^{3+}$ spectrum, where the lines D′ and D are better resolved.

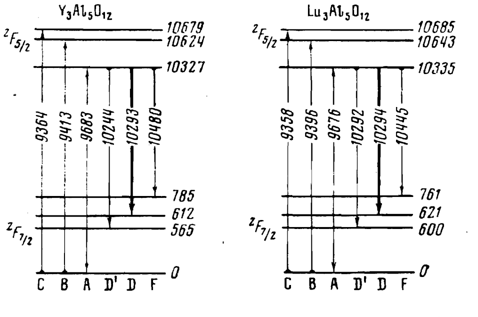

FIG. 3. Crystalline splitting of the multiplets $^2F_{5/2}$ and $^2F_{7/2}$ of the ion Yb^{3+} in $Y_2Al_5O_{12}$ and $Lu_3Al_5O_{12}$ crystals at 77°K. The level positions are in cm^{-1} and the wavelengths of the transitions between them in Å. The induced transitions are marked by thick arrows.

The line D′ was not taken to be a ZPL in any of the cited papers. In addition to the already presented arguments favoring its electronic origin, we point out that its intensity is comparable with the intensity of the D line and clearly exceeds the average intensity of the EVS. There is no doubt that the lines D′ and D belong to activator centers of the same type, since the ratio of their intensities does not vary with the ytterbium concentration.

In the luminescence spectra, the line D is followed by a relatively weak structure that extends to ≈ 860 cm^{-1}. The nature of lines E, E′ and E″ of this structure is not quite clear. It is possible that they are due to transitions in which two phonons take part. Thus, the appearance of the E′ line may be due to phonons of energy 320 and 380 cm^{-1}, the E′ line to 320 and 400 cm^{-1} phonons, and the E″ line to 380 and 400 cm^{-1} phonons. The intensities of these two phonon peaks turn out to be comparable with the intensity of the one-phonon lines, possibly because they are on the wing of the broad zero-phonon line F. We note, in addition, that all the cited energies correspond to sharp and intense phonon-density peaks.

2. Radiative transition probabilities. To calculate the SE parameters of laser crystals it is necessary to know the "Stark" luminescence branching coefficients β_{ij}, and the probabilities or the effective cross sections σ_e of radiative transitions from individual levels of the metastable state. It is desirable to obtain this information also for another reason: an investigation of the radiative-transition probabilities with the Nd^{3+} ion as an example[30] has shown that they are arranged in an interesting systematic sequence and make it possible to predict the spectral properties of a medium activated by a given ion.

The electron-vibrational structure of the luminescence spectrum makes it difficult to determine the above-mentioned quantities and allows us in our case only to make estimates that cannot claim high accuracy. In Table II are given the values of β_{ij} and A_{ij} for the transitions between the Yb^{3+} levels, obtained at 77°K. The line marked EVS-I lists the total probabilities of the electron-vibrational transitions in which low-frequency phonons ($\hbar\omega_{ph} < 300$ cm^{-1}) take part; line EVS-II lists the same quantities for transitions in which high-frequency phonons participate ($300 < \hbar\omega_{ph} < 560$ cm^{-1}); line EVS-III gives the same for the transitions corresponding to lines E, E′, and E″.

The coefficients β_{ij} were determined as the areas under the corresponding contours, normalized to the area of the entire spectrum. The probability of line A was estimated from the absorption spectra. The broadening of line A at 77°K is inhomogeneous. It depends on the activator concentration and amounts to 1–2 cm^{-1}. The homogeneous component predominates at 77°K in

TABLE II. Spectral characteristics and intensities of the luminescent transitions of Yb^{3+} ions in $Y_3Al_5O_{12}$ and $Lu_3Al_5O_3$ crystals at 77°K.

Lines	$Y_3Al_5O_{12}$			$Lu_3Al_5O_{12}$		
	A_{ij}, sec^{-1}	β_{ij},	σ_e, 10^{-19} cm^2	A_{ij}, sec^{-1}	β_{ij},	σ_e, 10^{-19} cm^2
ZPL A	80–120	≈0,11	1,7 *	120–160	≈0.13	1.5 *
EVS-I	20	0.23 **	–	20	0.20 **	–
EVS-II	170	–	–	160	–	–
ZPL D′	140	0.16	0.33	150	0.15	0.26
ZPL D	420	0.47	1.4	460	0.46	1.8
EVS-III	30	–	–	20	–	–
ZPL F	30	0.03	0.04	60 ***	0.06	0.05

---

*The presented values of σ_e of line A were obtained at $\Delta\nu_{lum}=1.3$ cm^{-1} for $Y_3Al_5O_{12}$: Yb^{3+} (≈3 at.%) and at $\Delta\nu_{lum}=2.0$ cm^{-1} for $Lu_3Al_5O_{12}$: Yb^{3+} (≈2 at.%).

**Summary luminescence branching coefficient for electron-vibrational transitions.

***In the $Lu_3Al_5O_{12}$: Yb^{3+} crystal, the EVS line E″ is at resonance with the zero-phonon line F. In contrast to $Y_3Al_5O_{12}$: Yb^{3+}, they cannot be separated even approximately. This explains the substantial difference of the behaviors of this line in the two crystals.

the broadening of the remaining ZPL lines, which were assumed in the calculations to have a Lorentz shape. In the determination of β_{ij}, the lines D′ and D in the luminescence spectrum of $Y_3Al_5O_{12}$ were separated graphically under the assumption that the contribution of the latter to the combined contour is small at the points on the long-wave side of the maximum of D, and that the line D is symmetric in shape. The same procedure was used to separate the lines E′ and F in $Lu_3Al_5O_{12}:Yb^{3+}$, and the lines E″, F, D″ and the EVS lines in $Y_3Al_5O_{12}:Yb^{3+}$: In all cases, the difference between the sum of the areas of the separated lines and the area bounded by the initial contour was less than 5%.

3. Luminescence lifetime of Yb^{3+} ions. The temperature dependences of τ_{lum} of the $^2F_{5/2}$ state in both investigated crystals are shown in Fig. 4. The increase of the lifetime with temperature can be due to two causes. The first is the enhancement of the reabsorption of the luminescence following temperature-induced population of the excited Stark components of the ground state; the second is the redistribution of the population of the upper multiplet among its Stark components under the condition that the probabilities of the radiative transitions from the two upper levels are smaller than the probability of the transitions from the lower component.

The data shown in Fig. 4 were obtained under conditions when the influence of the first cause is excluded (low activator concentration, thin crystal layer). In the absence of nonradiative transitions, the value of τ_{lum} for the state $^2F_{5/2}$ is determined from the expression

$$1/\tau_{lum}=A_1N_1+(A_2+A_3)N_{2,3}, \qquad (6)$$

where N_i are the populations of the Stark components divided by the population of the entire multiplet, $N_2 \approx N_3 = K_{2,3}$. At low temperatures the value of τ_{lum} is determined by the probability A_1. The change of τ_{lum} with increasing temperature manifests itself most noticeably up to $kT_1 \sim E_{2,3} - E_1$. At higher temperatures both the growth of $N_{2,3}$ and the change of τ_{lum} slow down. The value of kT_1 determined from the data of Fig. 4 is close to the magnitude of the Stark splitting of the $^2F_{5/2}$ state.

From the shapes of the experimental plots of $\tau_{lum}(T)$ we can estimate the total probability of radiation from the two upper levels of $^2F_{5/2}$. Such an estimate yields $A_2 + A_3 = 770$ sec^{-1} for the $Y_3Al_5O_{12}:Yb^{3+}$ crystal and 1270 sec^{-1} for $Lu_3Al_5O_{12}:Yb^{3+}$. The average probability for each of the eight transitions that start with the upper levels of the $^2F_{5/2}$ multiplet is thus relatively small. It must be noted here that the slowing down of the growth of τ_{lum} at high temperatures can also be due to the increased intensity of the EVS if the presence of the latter is due to any degree to the fact that the transition $^2F_{5/2} \longrightarrow {}^2F_{7/2}$ is made vibrationally allowed. In our case, the contribution of this mechanism cannot apparently be significant, since the position of the Yb^{3+} in the aluminum garnet does not have an inversion center and the electrodipole transition between the ^2F_J multiplets is made allowed mainly by the odd components of the static part of the crystal field.

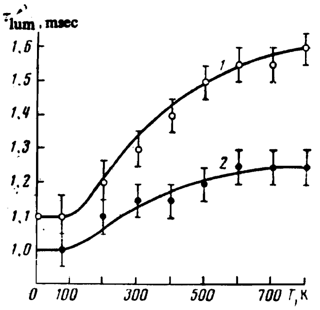

FIG. 4. Temperature dependences of the luminescence lifetime of the $^2F_{5/2}$ state of Yb^{3+} ions in the crystals $Y_3Al_5O_{12}$ (1) and $Lu_3Al_5O_{12}$ (2). Solid lines—calculation of $\tau_{lum}(T)$ by formula (6).

4. Results of the investigation of stimulated emission. The production of SE of Yb^{3+} in garnets has certain distinguishing features. Even though the paucity of the spectrum of the electronic transitions of Yb^{3+} is offset in part by the EVS, the values of E_{thr} remain relatively high and limit the range of measurements of the lasing parameters of these crystals to low temperatures (up to ≈170°K). The efficiency of excitation of the SE of Yb^{3+} ions in garnets by broad-band pumping sources (lamps of the IFP type) is substantially enhanced if the absorption bands of coactivator ions (sensitizers) are used, especially Nd^{3+} and Cr^{3+}.[1,3,4,6] Excitation from the metastable states of the latter is transferred by nonradiative means to the Yb^{3+} ions, thus appreciably lowering their lasing threshold. Consequently, in the presence of co-activators it is possible to obtain SE at higher temperatures in crystals with Yb^{3+} ions. This is seen from the data shown in Fig. 5, where plots of $E_{thr}(T)$ are shown for three aluminum garnets. The SE spectra of two of them, at different temperatures, are shown in Fig. 6. Figure 7 shows plots of $\lambda_g(T)$. Other spectral and lasing parameters are listed in Table I.

The interpretation of the $E^*_{thr}(T)$ plots was carried out by using formula (1). Agreement between theory and experiment was attained by choosing the parameter C_0. The best agreement was obtained for $Lu_3Al_5O_{12}:Yb^{3+}$ at $C_0 = 1.4 \times 10^4$ cm^{-1}, for $Y_3Al_5O_{12}:Nd^{3+}-Yb^{3+}$ at $C_0 = 0.9 \times 10^4$ cm^{-1}, and for $Y_3Al_5O_{12}:Cr^{3+}, Nd^{3+}-Yb^{3+}$ at $C_0 = 1.3 \times 10^4$ cm^{-1}. These values agree well with the theoretical estimate $C_0 = 1.2 \times 10^4$ cm^{-1} obtained from formulas (2) at the following real values of the parameters: $\alpha = 1.5 \times 10^{-2}$ cm^{-1}, A = 520 sec^{-1}, and $N_0 = 1.3 \times 10^{20}$ cm^{-3} (for an Yb^{3+} concentration of about 1.0 at.%). Formula (1) describes satisfactorily the variation of $E_{thr}(T)$ only up to T ≈ 180°K. The deviation of the experimental values of E_{thr} from the values predicted by this formula at higher temperatures is attributed to the nonlinearity of the energy characteristic of the excitation lamp and to an increase in the absorption in the end sections of the crystal, which were inserted in holders and were not illuminated by the pump source.

It follows from Table I and Fig. 6 that for sensitized (Nd^{3+} or Nd^{3+} and Cr^{3+}) $Y_3Al_5O_{12}$ crystals, simultaneous lasing of the Yb^{3+} ions (on the D line) and Nd^{3+} ions (on the A and B lines of the $^4F_{3/2} \to {}^4I_{11/2}$ transition) is observed starting with ≈200°K. This effect was registered at an exciting-pulse duration ≈250 μsec and at E E_{exc}/E_{thr} = 2 to 2.5. In the case of low pump energies ($E_{exc} \approx E_{thr}$), the SE of the Yb^{3+} ions lags the lasing of the Nd^{3+} ions by approximately 50 μsec.

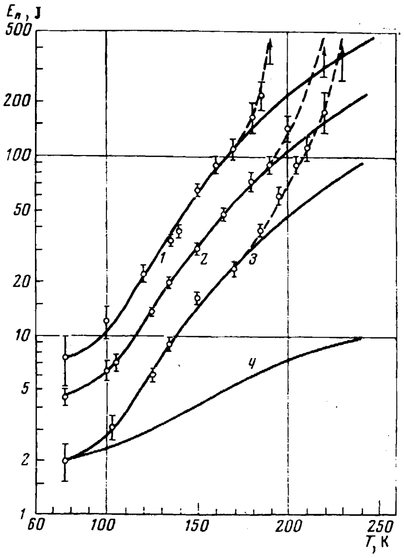

FIG. 5. Plot of $E_{thr}(T)$ of the D line for the following crystals: 1–$Lu_3Al_5O_{12}$–Yb^{3+}, 2–$Y_3Al_5O_{12}$: Nd^{3+}–Yb^{3+}, 3–$Y_3Al_5O_{12}$: Cr^{3+}, Nd^{3+}–Yb^{3+}. Dashed–experiment curves, solid–calculation by formula (1). The values of E_{thr} for $Lu_3Al_5O_{12}$: Yb^{3+} are magnified five times. Curve 4 shows the change of $\Delta\nu_{lum}$ (in relative units) of the lasing transition line of Yb^{3+} in $Y_3Al_5O_{12}$.

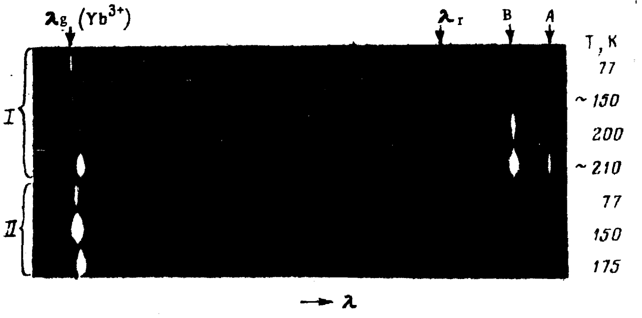

FIG. 6. Stimulated emission spectra of a laser based on the crystals I–$Y_3Al_5O_{12}$: Cr^{3+}, Nd^{3+}–Yb^{3+} ($^2F_{5/2} \to {}^2F_{7/2}$ for Yb^{3+} and $^4F_{3/2} \to {}^4I_{11/2}$ for Nd^{3+}) and II–$Lu_3Al_5O_{12}$: Yb^{3+} ($^2F_{5/2} \to {}^2F_{7/2}$) at various temperatures. The reference line with $\lambda_r \approx 10561$ Å is marked by an arrow.

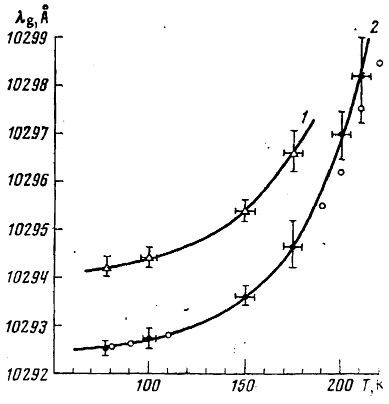

FIG. 7. Plots of $\lambda_g(T)$ of a laser based on the following crystals: 1–$Lu_3Al_5O_{12}$: Yb^{3+} and 2–$Y_3Al_5O_{12}$: Cr^{3+}, Nd^{3+}–Yb^{3+} (line D of the $^2F_{7/2} \to {}^2F_{7/2}$ transition). The light symbols show the change of the wavelength of the corresponding transition as obtained from luminescence data.

5. Temperature broadening and shift of the ZPL. The ZPL temperature broadening and shift due to the EPI was investigated in crystalline $Y_3Al_5O_{12}$: Yb^{3+}. We chose for this purpose the line A, which is sufficiently well isolated from the other lines. The experimental values of its width and shift relative to the position at 77°K are shown in Figs. 8 and 9. The change $\Delta\nu$ of the A line at T < 250°K follows quite well the plot of $\bar{n}(\omega_1)$, where ω_1 = 350 cm^{-1}. This fact confirms the existence of an electronic level of energy 10 679 cm^{-1}. To explain the variation of $\Delta\nu_{lum}(T)$ at T > 250°K it is necessary to take into account the contribution of the relaxation transitions between the levels of the lower multiplet. On the whole, the obtained variation of $\Delta\nu$ of the A line is satisfactorily described by the formula

$$\Delta\nu_{lum}(T) = 8.8[\bar{n}(\omega_1) + \bar{n}(\omega_2)] \quad [см^{-1}], \tag{7}$$

where ω_2 = 600 cm^{-1}.

No interpretation of the ZPL shift can be correct without a sufficiently convincing separation of that part of the shift which is due to the thermal expansion of the lattice. As the temperature is raised from 77 to 600°K, the lattice constant a_0 of $Y_3Al_5O_{12}$ increases by ≈0.04 Å.[31] The contribution of this change to the spectral-line shift can be estimated by comparing the positions of the Stark components of the Yb^{3+} ion in various garnets. In the homological series $TR_3Al_5O_{12}$ with TR = Y, Yb, and Lu, the value of a_0 decreases, viz., 12.01, 11.93, and 11.91 Å.[31,32] In the same sequence of crystals, the total splitting of the state $^2F_{7/2}$ is equal to 785, 766,[17] and 761 cm^{-1}, and the splitting of the $^2F_{5/2}$ multiplet remains practically unchanged. Thus, a decrease of a_0 by 0.1 Å is accompanied by an increase of the Stark splitting of one multiplet and does not affect the splitting of the other. Consequently, it does not cause a noticeable increase of the crystal potential at

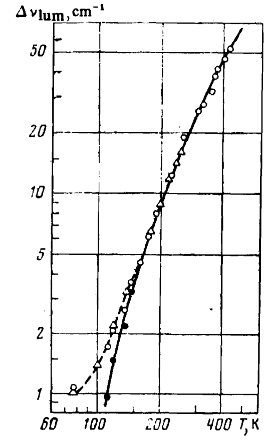

FIG. 8

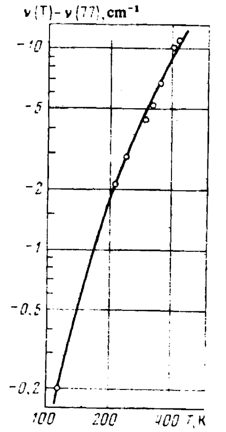

FIG. 9

FIG. 8. Temperature dependence of the width of line A ($^2F_{5/2} \to {}^2F_{7/2}$) in the $Y_3Al_5O_{12}$: Yb^{3+} crystal: ○–results of our experiment, ●–homogeneous broadening of the line A, △–experimental data of [13].

FIG. 9. Temperature dependence of the position of the line A ($^2F_{5/2} \to {}^2F_{7/2}$) in $Y_3Al_5O_{12}$: Yb^{3+} crystal. Solid curve–calculation by formula (8).

the location of the impurity ion, and the entire observed temperature shift of the ZPL of the Yb^{3+} ion in our crystal, in the entire indicated temperature interval, should be attributed to the influence of the EPI.

The experimental temperature dependence of the shift of line A agrees well with the theoretical curve described by the expression

$$\nu(T)-\nu(77\,K)=-28.5\bar{n}(\omega_3)\quad [\mathrm{cm}^{-1}], \tag{8}$$

where $\omega_3 = 400\ \mathrm{cm}^{-1}$. The luminescence spectrum (see Fig. 1) contains near this frequency the G lines of the EVS, and the intensities of these lines confirm the high activity of the interaction of the corresponding crystal vibrations with the impurity ions. There are grounds for assuming that the 400 cm^{-1} vibrations make the predominant contribution also to the temperature shifts of the spectral lines of the Nd^{3+} ion in $Y_3Al_5O_{12}$.[23] In accord with formula (5), upon interaction with the 400-cm^{-1} vibrations, the upper level of the transition A should move farther away from the other Stark components of the $^2F_{5/2}$ state, and the lower level of the same transition should come closer to the upper Stark components of the $^2F_{7/2}$ state. The presence of the EVS, unfortunately, does not make it possible to verify this conclusion, which explains the sign of the shift of the A line, at the required accuracy.

We have thus carried out, for the first time in a wide temperature interval, comprehensive spectral and lasing investigations of Yb^{3+} ions in crystals with garnet structure. Important information was obtained on the main physical phenomena that cause or accompany the SE effect in these media. The results of temperature measurements were interpreted in an approximate EPI model with allowance for the singularities of the distribution of the density of the impurity-active phonons in the aluminum garnets. The results presented in this paper offer evidence that garnet compounds with Yb^{3+} ions can be used as effective media in a laser of approximate wavelength 1.03 μ.

In conclusion, the authors thank Academician A. M. Prokhorov and Kh. S. Bagdasarov for a discussion of the results of the investigations of lasing by Yb^{3+} ions, T. T. Basiev and I. A. Shcherbakov for discussions on the migration of excitations in the investigated media, and A. M. Kevorkov, L. Li, A. G. Petrosyan, S. É. Sarkisov, and T. A. Tevosyan for supplying the crystals and taking part in the experiment.

---

[1] The probability of a nonradiative transition between states separated by an energy gap ≈1000 cm^{-1} is negligibly small in the laser crystals with TR^{3+} ions known to us.

[2] In the spectroscopic investigations we used also the $Yb_3Al_5O_{12}$ crystals.

[3] A detailed investigation of the EVS in the luminescence spectrum of Cr^{3+} in $Y_3Al_5O_{12}$ with separation of the structures R_1 and R_2 belonging to the ZPL is reported in [27].

[1] A. A. Kaminskiĭ, Lazernye kristally (Laser Crystals), Nauka, 1975.

[2] A. A. Kaminskiĭ, G. A. Bogomolova, and A. M. Kevorkov, Izv. Akad. Nauk SSSR, Neorg. Mater. 11, 884 (1975).

[3] Kh. S. Bargdasarov, G. A. Bogomolova, D. N. Vylegzhanin, A. A. Kaminskiĭ, A. M. Kevorkov, A. G. Petrosyan, and A. M. Prokhorov, Dokl. Akad. Nauk SSSR 216, 1247 (1974) [Sov. Phys. Dokl. 19, 358 (1974)].

[4] Kh. S. Bardasakov, A. A. Kaminskiĭ, A. M. Kevorkov, A. M. Prokhorov, S. E. Sarkisov, and T. A. Tovosyan, Dokl. Akad. Nauk SSSR 218, 550 (1974) [Sov. Phys. Dokl. 19, 592 (1975)].

[5] L. F. Johnson, J. E. Geusic, and L. G. Van Uitert, Appl. Phys. Lett. 7, 127 (1965).

[6] M. Robinson and C. K. Asawa, J. Appl. Phys. 38, 4495 (1967).

[7] H. F. Ivey, Proc. Internat. Conf. on Luminesc., Budapest, 1966, p. 2027.

[8] G. M. Zverev, I. I. Kuratev, and A. M. Onishchenko, Kvant. Élektron. (Moscow) 2, 469 (1975) [Sov. J. Quantum Electron. 5, 267 (1975)].

[9] T. T. Basiev, Yu. K. Voron'ko, T. G. Mamedov, V. V. Osiko, and I. A. Shcherbakov, in: Spektroskopiya kristallov (Spectroscopy of Crystals), Nauka, 1975, p. 155.

[10] V. V. Ovsyankin and P. P. Feofilov, Pis'ma Zh. Eksp. Teor. Fiz. 4, 471 (1967) [JETP Lett. 4, 317 (1967)].

[11] P. O. Feofilov, in: Fisika primesnykh tsentrov v kristallakh (Physics of Impurity Centers in Crystals), Izv. Akad. Nauk ESSR, Tallin, 1972, p. 539.

[12] L. F. Johnson, H. J. Guggenheim, T. C. Rich, and F. M. Ostermayer, J. Appl. Phys. 43, 1125 (1972).

[13] T. T. Basiev, Yu. Voron'ko, and I. A. Shcherbakov, Zh. Eksp. Teor. 66, 2118 (1974) [Sov. Phys.-JETP 39, 1042 (1974)].

[14] T. T. Basiev, Yu. K. Voron'ko, T. G. Mamedov, and I. A. Shcherbakov, Kvant. Élektron. (Moscow) 2, Nos. 11-12 (1975) [Sov. J. Quantum Electron. 5, Nos. 11-12].

[15] D. L. Wood, J. Chem. Phys. 39, 1671 (1963).

[16] J. A. Koningstein, Theoret. Chem. Acta, 3, 271 (1965).

[17] R. A. Buchanan, K. A. Wiekersheim, J. J. Pearson, and G. F. Herrmann, Phys. Rev. 159, 245 (1967).

[18] Y. Ayant and J. Thomas, C. R. Acad. Sci. (Paris) 248, 387 (1959).

[19] W. H. Brumage, C. C. Lin, and J. H. Van Vleck, Phys. Rev. 132, 608 (1963).

[20] M. T. Hutchings and W. P. Wolf, J. Chem. Phys. 41, 617 (1964).

[21] J. J. Pearson, G. F. Herrman, K. A. Wiekersheim, and R. A. Buchanan, Phys. Rev. 159, 251 (1967).

[22] Yu. E. Perlin and B. S. Tsukerblat, Éffekty elektron-kolebatel'nogo vzaimodeĭstviya v opticheskikh spektrakh primesnykh paramagnitnykh ionov (Effects of Electron-Vibrational Interaction in Optical Spectra of Impurity Paramagnetic Ions), Shtiintsa, Kishinev, 1974.

[23] I. S. Andriesh, V. Ya. Gamurar', D. N. Vylegzhanin, A. A. Kaminskiĭ, S. I. Klokishner, and Yu. E. Perlin, Kvant. Élektron. (Moscow) 2, 287 (1975) [Sov. J. Quantum Electron. 5, 162 (1975)].

[24] W. M. Yen, W. C. Scott, and A. L. Schawlow, Phys. Rev. 136A, 271 (1964).

[25] E. Cohen, L. A. Riseberg, and H. W. Moos, Phys. Rev. 175, 521 (1968).

[26] M. A. El'yashevich, Spektry redkikh, zemel' (Spectra of Rare Earths), Gostekhizdat, 1953, p. 401.

[27] I. N. Douglas, Phys. Status Solidi [a] 9, 635 (1972).

[28] L. A. Riseberg and M. J. Weber, Solid State Commun. 9, 791 (1971).

[29] B. F. Argyl, R. L. Wadsack, and R. K. Chang, J. Appl. Phys. 42, 1478 (1971).

[30] A. A. Kaminski and L. Li, Phys. Status Solidi [a] 26, 593 (1974); 26, K21 (1974).

[31] S. Geller, G. P. Espinosa, and P. B. Crandall, J. Appl. Cryst. 2, 86 (1969); W. J. Croft, Amer. Mineralogist 50, 1634 (1965).

Translated by J. G. Adashko
93